Inorganic Chemistry

Article

pubs.acs.org/IC

Oxorhenium(V) Complexes with Phenolate−Pyrazole Ligands for Olefin Epoxidation Using Hydrogen Peroxide

Niklas Zwettler, Jörg A. Schachner, Ferdinand Belaj, and Nadia C. Mösch-Zanetti*

Institute of Chemistry, University of Graz, Schubertstrasse 1, 8010 Graz, Austria

Supporting Information

ABSTRACT: Oxorhenium(V) complexes of the general formula $[ReOCl_2(PPh_3)(L)]$ (**2a−c**) and $[ReOCl(L)_2]$ (**3a−c**) with L being monoanionic, bidentate phenolate−pyrazole ligands **1a−c** that bear substituents with various electronic features on the phenol ring (**1a** Br, **1b** NO_2, **1c** OMe) were prepared. The compounds are stable toward moisture and air, allowing them to be handled in a normal lab atmosphere. All complexes were fully characterized by spectroscopic means and, in the case of **2b**, **2c**, **3b**, and **3c**, also by single-crystal X-ray diffraction analyses. Electrochemical investigations by cyclic voltammetry of complexes **3a−c** showed a shift to more positive potentials for the Re(V)/Re(VI) redox couple in the order of **3b** > **3a** > **3c** (R= NO_2 > Br > OMe), reflecting the higher electrophilic character of the Re atom caused by the ligands **1a−c**. Complexes **2a−c** and **3a−c** display excellent catalytic activity in the epoxidation of cyclooctene, where all six complexes give quantitative conversions to the epoxide within 3 h if *tert*-butylhydroperoxide (TBHP) is employed as oxidant. Moreover, they represent rare examples of oxorhenium(V) catalysts capable of using the green oxidant hydrogen peroxide, leading to high yields up to 74%. Also, green solvents such as diethylcarbonate can be used successfully in epoxidation reactions, albeit resulting in lower yields (up to 30%).

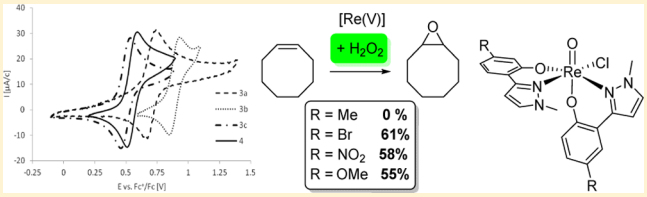

INTRODUCTION

Olefin epoxidation has been intensely investigated for many years, and catalysts containing rhenium in its highest oxidation state of +VII were of special interest.[1−7] Among them, the rhenium(VII) catalyst methyltrioxorhenium (MTO) was identified as a very potent catalyst for olefin epoxidation.[3,4,6−9] Despite its high catalytic activity and broad applicability, MTO is accompanied by a few drawbacks. A disadvantage is the substrate scope, which is sometimes hampered by the acidity of the MTO/H_2O_2 system, which can cause ring-opening of the formed epoxide. This problem has been overcome by the addition of Lewis bases such as pyridine and pyrazole.[5,9−12] Another disadvantage is that such Lewis base adducts based on MTO are sometimes more water-sensitive than MTO itself and are therefore vulnerable to decomposition.[11−13] This limits the catalyst lifetime when hydrogen peroxide is used as oxidant because H_2O is formed as a side product.[1,9,14] Thus, regardless of the impressive success of MTO as an epoxidation catalyst, the development of new rhenium catalysts with improved properties represents a worthwhile goal.

Rhenium(V) complexes, initially investigated for their role in oxygen-atom transfer reactions,[15] have found use as moisture-stable catalysts in some epoxidation reactions.[16−23] In early investigations, such compounds coordinated by bidentate or tetradentate Schiff base ligands were found to catalyze the epoxidation of cyclooctene with *tert*-butylhydroperoxide (TBHP) and gave yields of up to 66%. Also, oxorhenium(V) complexes with pyridylalkoxide ligands showed catalytic activity in olefin oxidation but only up to 30% conversion.[18] Furthermore, when substituted by only one pyridylalkoxide, the complexes partially decomposed to perrhenate ions and free ligand.[18] Phenolate pyrazole ligands are known to be good donor groups for rhenium(V) complexes.[24] We used a series of Re(V) complexes coordinated by phenolate- and naphtholate-pyrazole ligands as catalysts in the epoxidation of cyclooctene, yielding between 49 and 64% of cyclooctene epoxide with *tert*-butylhydroperoxide (TBHP) as oxidant in 120 min without an induction period.[21] Comparison of the naphthol- and phenol-based ligands and their very similar behavior in catalysis indicated that steric properties of the aromatic moiety have little influence on catalyst activity.[21] In all of the above-described systems, TBHP was used as oxidant. A rare example of an oxorhenium(V) catalyst that showed epoxidation activity with H_2O_2 was found to be the mono-oxo methyl substituted Re(V) complex equipped with two picolinato ligands. However, the two-phase system required 150 equiv of H_2O_2.[17]

The generally favorable features of the oxorhenium(V) complexes, such as convenient synthesis, large scope of possible ligands, and easy handling due to moisture and oxygen stability but with still improvable catalytic properties, prompted us to further investigate our phenolate−pyrazole systems. Therefore, we decided to activate the complexes by introducing electron-withdrawing and/or polar groups R in the ligand backbone (**1a**, R = Br; **1b**, R = NO_2; **1c**, R = OMe) in contrast to ligands bearing electron donating and apolar substituents.[21]

Received: July 28, 2014
Published: December 2, 2014

   dx.doi.org/10.1021/ic501794z | *Inorg. Chem.* 2014, 53, 12832−12840

Scheme 1. (Left) Two-Step Synthesis of Ligands 1a−c from Hydroxyacetophenone and (right) Alternative One-Step Synthesis of 1b from Commercially Available Nitrochromone[25]

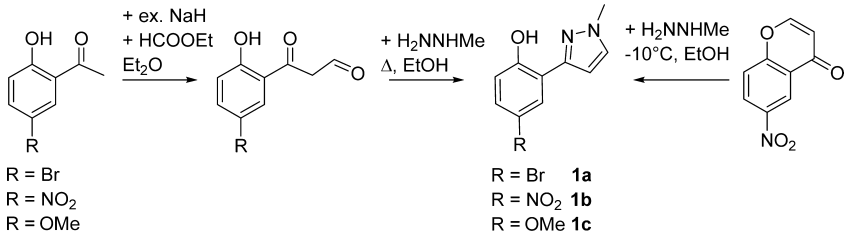

Here, we report a set of phenolate−pyrazole ligands **1a−c** with polar and/or electron-withdrawing groups (**1a** = Br, **1b** = NO_2, **1c** = OMe) in *para* position on the phenolate ring and the respective mono- and disubstituted oxorhenium(V) complexes of the general structures $[ReOCl_2(PPh_3)(L)]$ (**2a−c**) and $[ReOCl(L)_2]$ (**3a−c**). Their catalytic behavior in epoxidation reactions of cyclooctene with TBHP and H_2O_2 under various conditions are described.

RESULTS AND DISCUSSION

Ligand Synthesis. Ligands **1a−c** were prepared according to Scheme 1. Phenolate−pyrazole ligands have been previously published by different synthetic routes.[25−28] For **1a**, we found a modified procedure that is shorter by three steps in comparison to the published one.[28] Ligand **1b** can be prepared in a single step because 6-nitrochromone is commercially available (Scheme 1).[25] Alternatively, the synthesis of **1b** can also be accomplished starting from the cheaper 2′-hydroxy-5′-nitroacetophenone via our modified route in two steps. Furthermore, by using an excess of sodium hydride (60% dispersion in mineral oil) instead of sodium powder,[26] the syntheses can be performed conveniently under atmospheric conditions.[21] The addition of excess formic acid ethyl ester to the deprotonated hydroxyacetophenone forms the hydroxyphenyl oxopropanal species, which is used directly in the next step. This *β*-ketoaldehyde can undergo an intramolecular ring condensation to form a chromone (Scheme 1).[29] The addition of methylhydrazine to the *β*-ketoaldehyde (Scheme 1, left) or the commercially available chromone (Scheme 1, right) species and heating leads to the desired pyrazole ligands **1a−c**.

Ligands **1a−c** were purified by column chromatography. The overall yield of this two-step reaction is between 38 and 45%, depending on the R-group (**1a**, 42%; **1b**, 38%; **1c**, 45%). When the commercially available nitrochromone was used for the synthesis of **1b**, a significantly higher yield of 75% was obtained.

Synthesis of Monosubstituted Complex. The use of the oxorhenium(V) precursor $[ReOCl_3(PPh_3)_2]$[30] leads selectively to monosubstituted complexes, as we have previously observed.[21] For the complex synthesis, open flask procedures and commercial grade solvents can be used because complexes **2a−c** are stable toward moisture and oxygen (Scheme 2).

A slight excess of ligand and the metal precursor were dissolved in acetonitrile and heated for 4 h. Upon heating the mixture to reflux temperature, the solution turned dark green, indicating the formation of complexes. After the solution was cooled and concentrated, complexes **2a−c** started to precipitate as dark green microcrystalline, analytically pure solids. Recrystallization from CH_2Cl_2 gave single crystals of **2a** and **2b** suitable for single crystal X-ray diffraction analysis (vide infra). Complexes **2a−c** are only sparingly soluble in polar solvents (e.g., $CHCl_3$, CH_2Cl_2, CH_3CN, THF) and nonsoluble

Scheme 2. Synthesis of Monosubstituted Oxorhenium(V) Complexes 2a−c

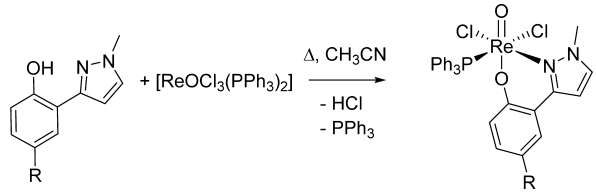

in apolar solvents. Proton and phosphor NMR spectroscopy indicated the formation of monosubstituted complexes with one coordinated phenolate−pyrazole ligand and one coordinated phosphine ligand. No decomposition in the solid state or in solution was observed over a prolonged time.

Synthesis of Disubstituted Complexes. For the synthesis of disubstituted Re complexes, the metal precursor $(NBu_4)[ReOCl_4]$[31] was used. Heating a solution of the respective ligand and $(NBu_4)[ReOCl_4]$ in commercial grade MeOH resulted in a dark green coloration of the solution, indicating the formation of complexes. Upon concentration to a small volume and storage at −25 °C, crystallization of the respective disubstituted complex **3a−c** occurred in good yields. The obtained green solids are stable to air and moisture. No decomposition in the solid state or in solution was observed over a prolonged time. Complexes **3a−c** are only sparingly soluble in polar solvents (e.g., $CHCl_3$, CH_2Cl_2, CH_3CN, THF) and nonsoluble in apolar solvents. Proton NMR spectroscopy indicated the formation of disubstituted complexes with two coordinated pyrazole ligands. Due to the lack of symmetry, the two ligands gave two different sets of signals. For complex **3c**, four different signals for the four methyl groups were observed between 3 and 5 ppm (CD_3CN). It is interesting to note that for ligands **1a−c**, no addition of a base was needed to synthesize complexes **3a−c**. This is in contrast to the synthesis of previously published disubstituted complexes (e.g., **4**, R = Me, Scheme 3) in which the addition of a base (e.g., NaH) was necessary to induce complex formation.[21]

Molecular Structures. Molecular structures of monosubstituted complexes **2b** and **2c** and disubstituted complexes **3b** and **3c** were obtained by single-crystal X-ray diffraction analysis. Crystallographic data and structure refinements for all four compounds are summarized in Table 1. Molecular views of **2b** and **2c** are given in Figure 1, those of **3b** and **3c** are given in Figure 2. Selected bond angles and lengths for **2b−c** are given in Table 2, and those for **3b−c** are given in Table 3. In general, all bond angles and distances are as expected and within the range of previously reported oxorhenium(V) com-

dx.doi.org/10.1021/ic501794z | Inorg. Chem. 2014, 53, 12832−12840

Scheme 3. Synthesis of Disubstituted Complexes 3a−c

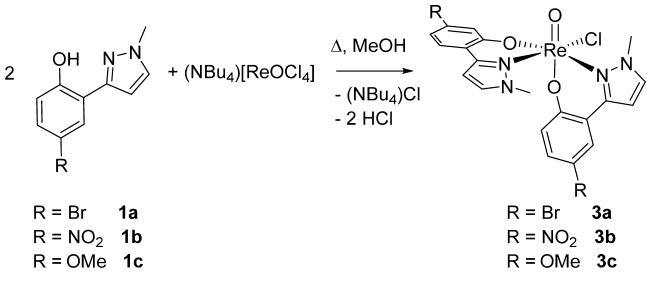

plexes.[19,20,23,32] It is interesting to note that none of the four structurally characterized complexes show significant deviations in the solid state structure concerning bond distances or angles in comparison to previously published complexes without electron-withdrawing pyrazole ligands.[21,33]

In complexes **2b** and **2c**, the rhenium atoms are coordinated in a distorted octahedral fashion by the bidentate pyrazole ligand and in a monodentate fashion by the phosphine, the terminal oxo and the two chloro ligands. The phosphine and one chloro ligand occupy the axial positions. Similar to other published complexes, the terminal oxo ligand O1 is in *trans* position to the phenolato oxygen atom, and the N12 atom of the pyrazole ring is in *trans* orientation to the second chloro ligand.[21,34]

Also in complexes **3b** and **3c**, the central rhenium atoms are coordinated in a distorted octahedral fashion by the two bidentate pyrazole ligands, a terminal oxo and a chloro ligand. The bidentate pyrazole ligands coordinate in an asymmetric motif, with one ligand occupying two equatorial positions and the other ligand occupying an equatorial and an axial position. Again, one phenolate oxygen is located trans to the terminal oxo ligand, and the two nitrogen donor atoms of the pyrazole units are located *cis* to each other. This type of asymmetric coordination has also been observed in other disubstituted oxorhenium(V) complexes.[21,35]

Electrochemistry. To probe the electronic influence of ligands **1a−c** on the metal center, we performed cyclic voltammetry experiments on complexes **3a−c** and compared the obtained redox potentials to the redox potential of the previously published complex **4** (R = Me).[21] Whereas complexes **3a−b** displayed the electrochemistry of quasi-reversible redox couples, the cyclic voltammogram of complex **3c** was more complex and showed several irreversible faradaic processes (Supporting Information). These additional irreversible peaks are also observed in the cyclic voltammogram of ligand **1c** and are therefore most likely caused by irreversible oxidations/reductions of the ligand backbone. Nevertheless, the quasi-reversible metal-centered redox couples could be clearly identified for **3c**. All three complexes **3a−c** displayed two quasi-reversible redox couples E^0_1 and E^0_2 corresponding to the Re(V)/(VI) and Re(IV)/(V) redox couple, respectively (Table 4). On the basis of the peak height and by comparison to literature results, we assigned the redox couples at positive potentials to the Re(V)/Re(VI) couple.[36]

Table 1. Crystallographic Data and Structure Refinement for Complexes 2b−c and 3b−c

	2b	3b	2c	3c
empirical formula	$C_{28}H_{23}Cl_2N_3O_4PRe$	$C_{20}H_{16}ClN_6O_7Re{\cdot}C_2H_3N$	$C_{29}H_{26}Cl_2N_2O_3PRe$	$C_{22}H_{22}ClN_4O_5Re$
formula weight	753.56	715.09	738.59	644.09
crystal size	0.25 × 0.22 × 0.16 mm	0.30 × 0.16 × 0.12 mm	0.28 × 0.25 × 0.10 mm	0.34 × 0.32 × 0.05 mm
crystal system, space group	triclinic, P1	monoclinic, C2/c	monoclinic, C2/c	monoclinic, $P2_1/c$
unit cell dimensions: a	9.3605(5)Å	27.3037(7)Å	12.2426(5)Å	11.2546(3)Å
unit cell dimensions: b	10.4113(5)Å	8.6888(2)Å	19.8120(9)Å	12.9161(4)Å
unit cell dimensions: c	14.5555(7)Å	22.8645(6)Å	22.8527(10)Å	15.0198(4)Å
unit cell dimensions: α	105.6595(16)°	116.2930(10)°	99.3430(10)°	90.4010(10)°
unit cell dimensions: β	99.0462(15)°			
unit cell dimensions: γ	95.7507(16)°			
volume	1333.60(12)Å^3	4863.1(2)Å^3	5469.4(4)Å^3	2183.31(11)Å^3
calculated density	1.877Mg/m^3	1.953Mg/m^3	1.794Mg/m^3	1.959Mg/m^3
Z	2	8	8	4
absorption correction	semiempirical from equivalents			
unit cell determination	2.23 < Θ < 30.73°	2.54° < Θ < 30.98°	2.48 < Θ < 30.99°	2.71 < Θ < 30.96°
	9801 reflections used at 100 K	9895 reflections at 100 K	9071 reflections used at 100 K	9978 reflections used at 100 K
Θ range for data collection	2.05−30.00°	1.66−30.00°	1.81−30.00°	2.08−30.00°
reflections collected/unique	25333/7758	27969/7108	35194/7984	15035/6297
significant unique reflections	7484 with I > 2σ(I)	6584 with I > 2σ(I)	7505 with I > 2σ(I)	5232 with I > 2σ(I)
R(int), R(sigma)	0.0249, 0.0228	0.0224, 0.0190	0.0223, 0.0169	0.0301, 0.0429
Completeness to Θ = 30.0°	99.7%	100.0%	99.9%	99.1%
refinement method	full-matrix least-squares on F^2			
data/parameters/restraints	7758/359/0	7108/353/0	7984/352/0	6297/310/0
goodness-of-fit on F^2	1.045	1.067	1.073	1.063
final R indices [I > 2σ(I)]	R1 = 0.0164, wR2 = 0.0408	R1 = 0.0155, wR2 = 0.0375	R1 = 0.0168, wR2 = 0.0411	R1 = 0.0299, wR2 = 0.0800
R indices (all data)	R1 = 0.0174, wR2 = 0.0413	R1 = 0.0179, wR2 = 0.0388	R1 = 0.0190, wR2 = 0.0421	R1 = 0.0416, wR2 = 0.0879
weighting scheme	w = $1/[\sigma^2(F_o^2) + (aP)^2 + bP]$ where $P = (F_o^2 + 2F_c^2)/3$			
weighting scheme parameters: a, b	0.0189, 0.9497	0.0167, 6.7850	0.0174, 11.6681	0.0404, 6.8391
largest Δ/σ in last cycle	0.002	0.002	0.007	0.002
largest difference peak and hole	1.517 and −1.099e/Å^3	1.115 and −0.896e/Å^3	1.097 and −1.110e/Å^3	1.856 and −1.950e/Å^3

dx.doi.org/10.1021/ic501794z | Inorg. Chem. 2014, 53, 12832−12840

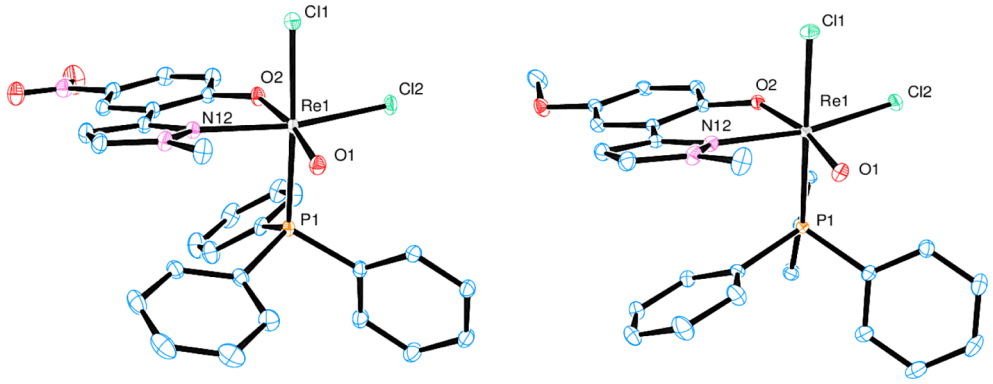

Figure 1. ORTEP plots of (left) **2b** and (right) **2c** showing the atomic numbering scheme. The probability ellipsoids are drawn at the 50% probability level. H atoms are omitted for clarity.

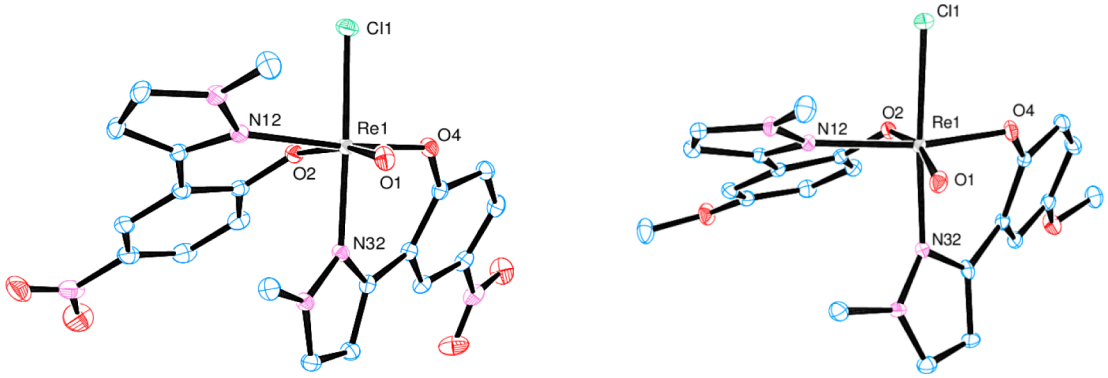

Figure 2. ORTEP plots of (left) **3b** and (right) **3c** showing the atomic numbering scheme. The probability ellipsoids are drawn at the 50% probability level. H atoms are omitted for clarity.

Table 2. Selected Bond Lengths (Å) and Angles (°) for Complexes 2b and 2c

	2b	2c
Re1−O1	1.6939(12)	1.6967(12)
Re1−O2	1.9378(12)	1.9232(12)
Re1−Cl1	2.4066(4)	2.4141(4)
Re1−Cl2	2.3648(4)	2.3681(4)
Re1−N12	2.1633(14)	2.1709(14)
Re1−P1	2.4708(5)	2.4784(4)
Cl1−Re1−P1	177.449(13)	179.709(15)

Table 3. Selected Bond Lengths (Å) and Angles (°) for 3b and 3c

3b		3c	
Re1−O1	1.6902(12)	Re1−O1	1.697(3)
Re1−O2	2.0015(12)	Re1−O2	1.947(3)
Re1−O4	1.9918(11)	Re1−O4	2.000(3)
Re1−N12	2.1187(14)	Re1−N12	2.142(3)
Re1−N32	2.1070(14)	Re1−N32	2.138(3)
Re1−Cl1	2.3563(4)	Re1−Cl1	2.3709(9)
N32−Re1−Cl1	168.01(4)	N32−Re1−Cl1	173.64(9)

The redox couples at negative potentials were therefore assigned to the Re(IV)/Re(V) couple. Analyte solutions for cyclic voltammetry were near 1 mM in acetonitrile, with $(NBu_4)PF_6$ used as supporting electrolyte (0.1 M). The cyclic voltammograms of **3a−c** and **4** are provided in the Supporting Information. To probe the electronic influence of the different ligands on the Re atom, we compared the redox couples at

Table 4. Redox Couples E^0_1 and E^0_2 Observed for Complexes 3a−c and 4

	E^0_1 (V)	E^0_2 (V)
3a	0.801	−1.54
3b	0.992	−1.30
3c	0.523	−1.82
4	0.568	−1.73

positive potentials for the Re(V)/Re(VI) couple of complexes **3a** (R = Br), **3b** (R = NO_2), and **3c** (R = OMe) with complex **4** (R = Me; Figure 3).

Oxidation/reduction processes were diffusion-controlled because peak potentials were independent of scan rates. Complexes **3a−b** displayed a shift to more positive potentials for the Re(V)/Re(VI) redox couple compared to **4**, demonstrating the higher electrophilicity of the Re atom. As expected, complex **3b** with R = NO_2 substituents is shifted the most to higher potentials compared to **4**. Complex **3c** (R = OMe) is shifted to a lower redox potential compared to **4**, reflecting the overall electron-donating nature of the methoxy group (methoxy group is a π-donor but σ-acceptor; the mesomeric +M effect is stronger than the inductive −I effect).[37] The order of increasing redox potentials is therefore **3c** < **4** < **3a** < **3b** (R = OMe < Me < Br < NO_2). The redox potentials also correlate well (R^2 = 0.9852) with the Hammett parameter σ^p (OMe = −0.268; Me = −0.170; Br = +0.232; NO_2 = +0.778; Figure 4) for para substituents.[38]

dx.doi.org/10.1021/ic501794z | *Inorg. Chem.* 2014, 53, 12832−12840

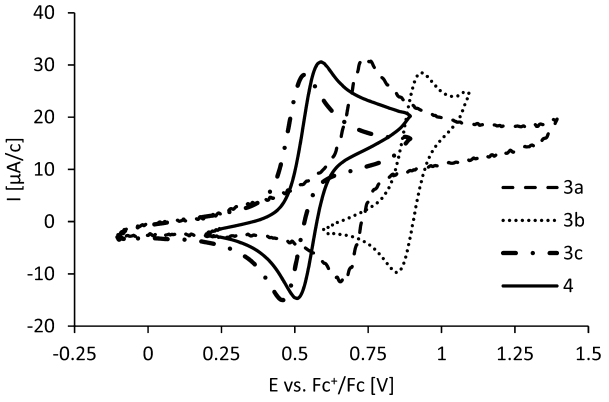

Figure 3. Comparison of Re(V)/Re(VI) redox couples of complexes **3a**–**c** and **4**. Cyclic voltammograms in acetonitrile, potential referenced to ferrocene and current normalized for concentration of analyte.

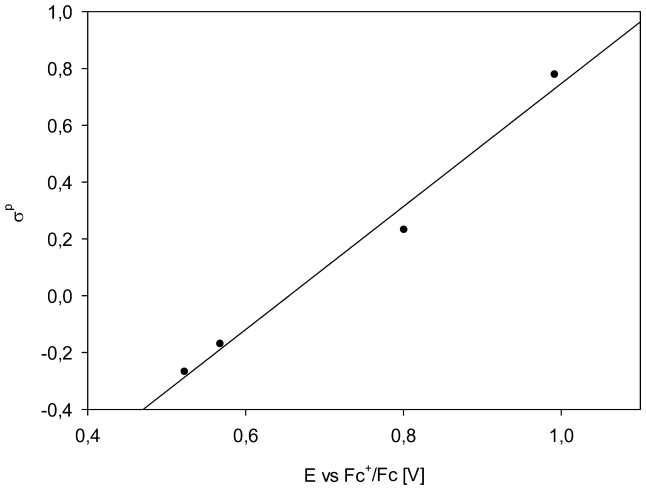

Figure 4. Correlation of redox potentials of complexes **3a**–**c** and **4** with Hammett parameter σ^p.

We also investigated the electrochemistry of complexes **2a**–**c**, but only several irreversible oxidation and reduction peaks were observed, which are likely due to decomposition reactions.

Catalytic Epoxidations. Complexes **2a**–**c** and **3a**–**c** were tested in the catalytic epoxidation of cyclooctene. A standard reaction was performed with 1 mol % of catalyst with 3 equiv of TBHP in $CHCl_3$ at 50 °C. As summarized in Table 5 and Figure 5, all complexes, with the exception or **3b**, show high activities. Monosubstituted complexes **2a**–**c** are slightly more active than disubstituted complexes **3a** and **3c**. Furthermore, all complexes were capable of epoxide formation between 92 and 97% with complete consumption of the substrate cyclooctene

Table 5. Yield (%) of Epoxide in the Re-Catalyzed Epoxidation of Cyclooctene with TBHP[a]

reaction time (h)	2a	3a	2b	3b[b]	2c	3c	4[c]
0	0	0	0	0	0	0	0
0.5	79	49	63	8	61	49	36
1.5	93	79	87	23	81	74	56
3	97	93	97	36	92	92	59

[a]Conditions: 1 mol % catalyst, 3 equiv of TBHP, 0.5 mL of $CHCl_3$, 50 °C. [b]Low solubility at 50 °C. [c]See reference 21.

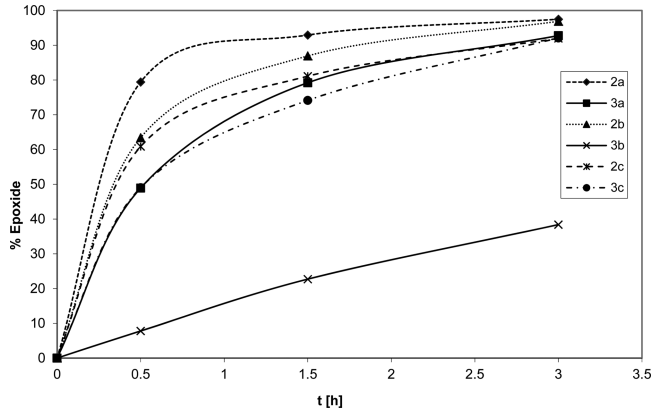

Figure 5. Yield of epoxide employing **2a**–**c** and **3a**–**c**. Conditions: 1 mol % catalyst, 3 equiv of TBHP, 0.5 mL of $CHCl_3$, 50 °C.

(below the threshold of the peak integration routine of the GC-MS software). This represents TOF numbers between 100 and 160 h^{-1}. The high observed conversion is noteworthy because with most previously described Re(V) catalysts, only up to 70% product formation was obtained, pointing to an increased stability of the catalysts here described.

A further interesting observation is that the catalytic reactions occur without an induction period for all six complexes despite the low solubility of the catalysts. Thus, at the on-set of the catalytic reaction, all complexes are only partially dissolved and dissolve quickly during the catalytic reaction. The lower activity of **3b** is most likely due to its poor solubility at 50 °C. Thus, this is the only compound where undissolved catalyst remains in the reaction mixture. If higher temperatures were applied (e.g., 80 °C in 1,2-dichloroethane), then **3b** also reached >95% yield of epoxide after 3 h. If the catalyst loading is reduced, then significantly lower epoxidation activities are observed. For example, if 0.1 mol % of **3c** is used at 50 °C, then only 20% epoxide is formed within 24 h. We also tested the more challenging substrates styrene and 1-octene, but under these conditions, no conversion to epoxides was observed. Nevertheless, for cyclooctene, the high yields of epoxide point to a generally higher stability of the complexes under oxidative reaction conditions.

To our delight, complexes **2a**–**c** and **3a**–**c** also proved to be active epoxidation catalysts with hydrogen peroxide as oxidant. In this case, standard catalytic experiments were performed in 1,2-dichloroethane at 80 °C with 1 mol % of catalyst and 3 equiv of H_2O_2 (30% in water), resulting in a two-phase system, and only the organic phase was colored.

All six complexes are active catalysts for the epoxidation of cyclooctene with H_2O_2. Within 1 h, between 42 and 52% of the olefin were converted to the epoxide. Thereafter, only small increases are observed. However, after 7 h, the selectivity started to drop, as indicated by the conversion of the epoxide formed to yet unidentified side products (the common side product cyclooctane-1,2-diol was not observed in the GC spectra). Complexes **2a**–**c** and **3a**–**c** also remain active when the amount of H_2O_2 is reduced to 1.5 equiv. For example, **2b** yields 38% epoxide after 3 h with 1.5 equiv of H_2O_2 (1 mol % **2b**, 1,2-dichlorethane, 80 °C). This is interesting and in stark contrast to the only other rhenium(V) complex reported to date capable of epoxidation with hydrogen peroxide where 150 equiv of the oxidant was necessary.[17] After prolonged reaction times, a discoloration of the reaction mixtures was observed,

dx.doi.org/10.1021/ic501794z | Inorg. Chem. 2014, 53, 12832–12840

hinting to catalyst decomposition.[18] Compound **4**, which has a methyl group in the backbone of the ligand, did not show any activity with hydrogen peroxide. Thus, the introduced polar substituent has a dramatic positive. Carbonate solvents are considered "green solvents" because they can be used to replace chlorinated solvents in many catalytic reactions.[39] Similar to the epoxidations in chlorinated solvents, the complexes do not dissolve completely at room temperature in carbonate solvents. Upon heating to 80 °C, the compounds dissolved completely. In diethylcarbonate (dec) catalyst **3c** converted 30% of cyclooctene using H_2O_2 after 7 h reaction time (Table 6).

Table 6. Yield (%) of Epoxide in the Re-Catalyzed Epoxidation of Cyclooocteene with H_2O_2[a]

reaction time (h)	2a	3a	2b	3b	2c	3c	4
1	52	53	47	55	50	42	0
3	54	55	53 (38)[c]	64	57	45	0
7	53	61	74	58	60	55 (30)[b]	0

[a]Conditions: 1 mol % catalyst, 3 equiv of H_2O_2, 0.5 mL of 1,2-dichloroethane, 80 °C. [b]Conversion in diethylcarbonate solvent. [c]1.5 equiv of H_2O_2.

This is significantly less than in 1,2-dichloroethane. At prolonged reaction times, the selectivity for cyclooctane epoxide dropped to 80%, with as yet unidentified side product formation.

Polar substituents have a dramatic positive effect. This is attributed to the increased polarity rather than the electron-withdrawing effect. Of particular interest for rationalization is the result of compound **3c** that is coordinated by the methoxy-substituted ligand. According to the electrochemical investigation, the redox potentials of **3c** and **4** are largely similar; however, their catalytic behavior is not.[21] Using H_2O_2, where the media is biphasic (H_2O and 1,2-$C_2H_2Cl_2$), the polar substituents might allow for reaction of the catalytic species with H_2O_2 across the phase boundaries, permitting the use of H_2O_2 as oxidant. In a previous investigation on the mechanism of TBHP catalyzed epoxidation with a Re(V) complex, we proposed a cationic trans-dioxorhenium species as a likely intermediate.[22] If a similar mechanism applies here, the polar substituents might facilitate the formation of such a charged species, resulting in the overall higher catalytic activity.

■ CONCLUSION

The introduction of polar substituents (R = Br **1a**, NO_2 **1b**, OMe **1c**) in the backbone of phenolate pyrazole ligands allows for the synthesis of oxorhenium(V) complexes **2a−c** and **3a−c** that are highly active in the epoxidation of cyclooctene. Upon using 1 mol % of the catalysts and three equiv of *tert*-butylhydroperoxide, complete conversions were observed, which is unique in Re(V) catalyzed epoxidation reactions. Moreover, these compounds are capable to catalyze the epoxidation of cyclooctene using the more challenging oxidant hydrogen peroxide. We attribute this enhanced epoxidation activity to the increased polarity of the complexes rather than the electron-withdrawing properties evidenced by cyclic voltammetry experiments, showing that the catalytic activity is independent of the redox potential of the Re center.

■ EXPERIMENTAL SECTION

Unless otherwise specified, all experiments were performed under atmospheric conditions with standard laboratory equipment. Commercially available chemicals and solvents were used as received, and no further purification or drying operations have been performed. Flash purifications were carried out on a Biotage Isolera ISO-4SV automatic flash purification system with UV detection at 254 and 280 nm. A gradient program was used with ethyl acetate and cyclohexane mixtures (5−100% of the ester) as eluent. The ^1H, ^{13}C, and ^{31}P NMR spectra were recorded on a Bruker Optics instrument at 300 MHz. Peaks are denoted as singlet (s), doublet (d), doublet of doublets (dd) and multiplet (m); "Ar" denotes aromatic protons; and "pyz" denotes pyrazole ring protons. Used solvents are mentioned at the specific data sets. The ^{13}C NMR spectra of complexes **2a−c** and **3a−c** could not be recorded due to the low solubility of the complexes. Electron impact mass spectroscopy (EI-MS) measurements have been performed with an Agilent 5973 MSD mass spectrometer with push rod. Results are denoted as cationic mass peaks, and the unit is the according ions mass/charge ratio. Gas chromatography mass spectroscopy (GC-MS) measurements have been performed with an Agilent 7890 A gas chromatograph (column type, Agilent 19091J-433), coupled to an Agilent 5975 C mass spectrometer. Samples for infrared spectroscopy were measured on a Bruker Optics ALPHA FT-IR Spectrometer. IR bands are reported with wavenumber (cm^{-1}) and intensities (vs, very strong; s, strong; m, medium; w, weak).

A Heidolph Parallel Synthesizer 1 was used for all epoxidation experiments. Electrochemical measurements were done under an inert Ar atmosphere in a glovebox in dry solvents with a Gamry Instruments Reference 600 Potentiostat using a three electrode setup. Glassy carbon was used as working electrode; Pt wire (99.99%) was used as supporting electrode; and the reference electrode was a Ag wire immersed in a solution of 0.01 M $AgNO_3$ and 0.1 M $(NBu_4)PF_6$ in CH_3CN separated from the solution by a Vycor tip. The supporting electrolyte used was $(NBu_4)PF_6$. IR compensation was applied. All elemental analyses were measured at the Graz University of Technology, Department of Inorganic Chemistry.

X-ray Crystal Structure Analysis. Structure determination of complexes **2b−c** and **3b−c** via X-ray diffraction analysis was performed on a Bruker-AXS Smart Apex CCD diffractometer. All the measurements were performed using graphite-monochromatized Mo K_α radiation at 100 K. The structures were solved by direct methods (SHELXS-97)[40] and refined by full-matrix least-squares techniques against F^2 (SHELXL-97).[40] The non-hydrogen atoms were refined with anisotropic displacement parameters without any constraints. The H atoms of the phenyl rings and of the pyrazol ring were put at the external bisectors of the X−C−C angles at C−H distances of 0.95 Å, and common isotropic displacement parameters were refined for the H atoms of the same ring. The H atoms of the methyl group were refined with a common isotropic displacement parameter and an idealized geometry with tetrahedral angles, enabling rotation around the N−C bond, and C−H distances of 0.98 Å.

Ligand Synthesis. *Synthesis of 4-Bromo-2-(1-methyl-1H-pyrazol-3-yl)phenol (**1a**).* The synthesis of this ligand has been previously published.[28] The procedure described here is shorter by three steps. Analytical data is consistent with published data. Sodium hydride (60% in mineral oil, 185 mg, 4.65 mmol, 5.0 equiv) and 1-hydroxy-5-bromo-acetophenone (200 mg, 0.93 mmol, 1.0 equiv) were dissolved in diethyl ether (60 mL), and the solution was stirred until no more hydrogen formation could be observed (indicated by a bubbler). Then, ethyl formate (0.63 mL, 9.30 mmol, 10 equiv) was added, and the reaction mixture was stirred in a water bath at 35 °C until the ether completely evaporated to obtain the intermediate 3-(2-hydroxy-5-bromophenyl)-3-oxopropanal. The unpurified 3-(2-hydroxy-5-bromophenyl)-3-oxopropanal was dissolved in ethanol ∼90% (100 mL, denatured with methanol, up to 7% H_2O), monomethylhydrazine (60 μL, 0.95 mmol, 1.2 equiv) was added, and the reaction mixture was stirred under reflux for 2 h. Purification of the reaction solution by column chromatography gave **1c** (99 mg, 42%) as brownish crystals.

*Synthesis of 4-Nitro-2-(1-methyl-1H-pyrazol-3-yl)phenol (**1b**).* A modification to a previously reported procedure for this ligand is described.[25] 6-Nitrochromone (400 mg, 2.08 mmol, 1.0 equiv) was dissolved in ethanol ∼90% (60 mL, denatured with methanol), monomethylhydrazine (0.13 mL, 2.50 mmol, 1.2 equiv) was added,

dx.doi.org/10.1021/ic501794z | Inorg. Chem. 2014, 53, 12832−12840

and the reaction mixture was stirred under reflux for 2 h. Purification of the crude product by column chromatography gave **1b** as a white, foamy solid (342 mg, 75%). ^{1}H NMR (300 MHz, chloroform-d) δ 11.74 (s, 1H, OH), 8.48 (d, J = 2.7 Hz, 1H, Ar), 8.10 (dd, J = 9.1, 2.7 Hz, 1H, Ar), 7.48 (d, J = 2.5 Hz, 1H, pyz), 7.07 (d, J = 9.1 Hz, 1H, Ar), 6.74 (d, J = 2.5 Hz, 1H, pyz), 3.99 (s, 3H, Me). ^{13}C NMR (75 MHz, chloroform-d) δ (ppm): 161.61, 149.62, 140.62, 131.79, 124.92, 122.56, 117.71, 117.12, 103.06, 39.30. EI-MS (m/z): 219.06 [M^+].

*Synthesis of 4-Methoxy-2-(1-methyl-1H-pyrazol-3-yl)phenol (**1c**).* Sodium hydride (1.20 g, 30.1 mmol, 5.0 equiv, 60% in mineral oil) and 1-hydroxy-5-methylacetophenone (1.00 g, 6.02 mmol, 1.0 equiv) were dissolved in diethyl ether (~60 mL), and the solution was stirred until no more hydrogen formation could be observed (indicated by a bubbler). Then, ethyl formate (4.10 mL, 60 mmol, 10 equiv) was added, and the reaction mixture was stirred in a water bath at 35 °C until the ether completely evaporated to obtain the intermediate 3-(2-hydroxy-5-methoxyphenyl)-3-oxopropanal. The unpurified 3-(2-hydroxy-5-methoxyphenyl)-3-oxopropanal was dissolved in ethanol 90% (100 mL, denatured with methanol), monomethylhydrazine (1.2 equiv, 0.38 mL, 7.2 mmol) was added, and the reaction mixture was stirred under reflux for 2 h. Purification of the crude product by column chromatography gave **1a** as a yellow crystalline solid (552 mg, 45%). ^{1}H NMR (300 MHz, chloroform-d) δ (ppm): 10.42 (s, 1H, OH), 7.38 (d, J = 2.4 Hz, 1H, pyz), 7.08 (d, J = 3.0 Hz, 1H, Ar), 6.95 (d, J = 8.9 Hz, 1H, Ar), 6.80 (dd, J = 8.9, 3.0 Hz, 1H, Ar), 6.57 (d, J = 2.4 Hz, 1H, pyz), 3.93 (s, 3H, OMe), 3.80 (s, 3H, Me). ^{13}C NMR (75 MHz, chloroform-d) δ (ppm): 152.61, 151.26, 150.02, 131.14, 117.61, 116.99, 114.90, 111.35, 102.46, 56.04, 39.26; IR: 2931.5 (w), 1625.8 (w), 1511.4 (m), 1486.2 (m), 1459.0 (m), 1280.1 (m), 1251.1 (m), 1203.1 (s), 1178.2 (m), 1041.3 (s), 812.6 (s), 757.9 (vs), 711.4 (s), 667.0 (m), 586.4 (w) . EI-MS (m/z): 204.1. [M^+]. Anal. calcd for $C_{11}H_{12}N_2O_2$ (204.23): C, 64.69; H, 5.92; N, 13.72. Found: C, 64.48; H, 5.82; N, 12.84.

Complex Synthesis. *Synthesis of [ReOCl$_2$(PPh$_3$)(**1a**)] (**2a**).* Ligand **1a** (25 mg, 0.10 mmol, 1.2 equiv) was dissolved in acetonitrile (~20 mL), then [ReOCl$_3$(PPh$_3$)$_2$] (80 mg, 0.08 mmol, 1.0 equiv) was added to the reaction mixture, and the mixture was stirred under reflux for 4 h. After the mixture cooled to room temperature, the solvent was reduced to a small amount (~4 mL) upon which crude material of **2a** precipitated. Recrystallization of the green residue from acetonitrile gave **2a** as a brownish green powdery solid (35 mg, 54%). ^{1}H NMR (300 MHz, acetonitrile-d3) δ 7.70 (d, J = 2.9 Hz, 1H, pyz), 7.50−7.28 (m, 15H, PPh$_3$), 7.24 (d, J = 2.5 Hz, 1H, Ar), 7.02 (dd, J = 8.8, 2.5 Hz, 1H, Ar), 6.66 (d, J = 2.9 Hz, 1H, pyz), 6.59 (d, J = 8.8 Hz, 1H, Ar), 4.08 (s, 3H, Me). (Acetonitrile-d3, 121 MHz) δ (ppm): −23.23 ppm. IR (cm^{-1}): 3121.8 (w), 1516.3 (m), 1480.2 (m), 1433.9 (m), 1397.0 (m), 1290.1 (m), 1094.7 (m), 954.4 (m), 879.2 (m), 816.5 (m), 745.0 (s), 692.1 (vs), 527.4 (s), 509.6 (s), 495.7 (s), 414.2 (m). EI-MS (m/z): 707.2 [M^+ − Br], 526.0 [M^+ − PPh$_3$]. Anal. calcd for $C_{28}H_{23}BrCl_2N_2O_2PRe$ (787.49): C, 42.71; H, 2.94; N, 3.56. Found: C, 41.26; H, 2.74; N, 3.41.

*Synthesis of [ReOCl(**1a**)$_2$] (**3a**).* Ligand **1a** (14 mg, 0.04 mmol, 2.1 equiv) was dissolved in MeOH (~10 mL), then (NBu$_4$)[ReOCl$_4$] (20 mg, 0.02 mmol,1.0 equiv) was added, which resulted in the immediate formation of green precipitate. The reaction solution was stirred under reflux for 4 h. After the mixture cooled to room temperature, **3a** precipitated as a green solid and was isolated by filtration. Recrystallization of the precipitate from MeOH gave **3a** as a bright green powder (11 mg, 72%). ^{1}H NMR (300 MHz, acetonitrile-d3) δ 7.98 (d, J = 2.8 Hz, 1H, pyz), 7.92 (d, J = 2.5 Hz, 1H, Ar), 7.76 (d, J = 2.5 Hz, 1H, Ar), 7.56−7.50 (m, 2H), 7.12 (d, J = 8.8 Hz, 1H, Ar), 7.09 (dd, J = 8.8, 2.5 Hz, 1H, Ar), 7.00 (d, J = 2.8 Hz, 1H, pyz), 6.82 (d, J = 2.8 Hz, 1H, pyz), 5.98 (d, J = 8.8 Hz, 1H, Ar), 4.46 (s, 3H, Me), 3.33 (s, 3H, Me). IR: 3142.5 (w), 1515.4 (m), 1477.7 (m), 1453.2 (m), 1397.1 (m), 1278.6 (s), 1221.7 (m), 1140.7 (m), 1075.9 (m), 954.5.2 (vs), 861.7 (m), 837.3 (m), 734.7 (s), 651.9 (m), 607.3 (m), 544.1 (m), 411.3 (m). EI-MS (m/z): 742.3 [M^+]. Anal. calcd for $C_{20}H_{16}Br_2ClN_4O_3Re$ (741.83): C, 32.38; H, 2.17; N, 7.55. Found: C, 32.74; H, 2.16; N, 7.40.

*Synthesis of [ReOCl$_2$(PPh$_3$)(**1b**)] (**2b**).* Ligand **1b** (60 mg, 0.27 mmol, 1.2 equiv) was dissolved in acetonitrile (~30 mL), and [ReOCl$_3$(PPh$_3$)$_2$] (183 mg, 0.22 mmol, 1.0 equiv) was added. The suspension was stirred under reflux for 4 h, upon which the mixture turned dark green. After the mixture cooled to room temperature, the solvent was reduced to a small amount (~10 mL) upon which crude material of **2b** precipitated. Recrystallization of the crude material from acetonitrile gave **2b** as deep green crystals suitable for X-ray crystallography (114 mg, 69%). ^{1}H NMR (300 MHz, acetonitrile-d3) δ (ppm): 7.92 (d, J = 2.9 Hz, 1H, pyz), 7.76 (d, J = 2.9 Hz, 1H, pyz), 7.73 (dd, J = 9.1, 2.9 Hz, 1H, Ar), 7.53−7.26 (m, 15H, PPh$_3$), 6.80 (d, J = 2.9 Hz, 1H, Ar), 6.78 (d, J = 9.1 Hz, 1H, Ar), 4.10 (s, 3H, Me). ^{31}P NMR (acetonitrile-d3, 121 MHz) δ (ppm): −23.65 ppm. IR (cm^{-1}): 3125.4 (w), 1503.2 (m), 1434.0 (m), 1324.1 (s), 1300.5 (s), 1281.6 (s), 1125.0 (m), 1095.5 (m), 962.9 (s), 886.5 (s), 742.7 (s), 683.4 (vs), 527.7 (vs), 511.3 (s), 493.6 (m). EI-MS (m/z): 718.4 [M^+ − Cl]. Anal. calcd for $C_{28}H_{23}Cl_2N_3O_4PRe$ (753.59): C, 44.63; H, 3.08; N, 5.58. Found: C, 45.18; H, 3.12; N, 5.65.

*Synthesis of [ReOCl(**1b**)$_2$] (**3b**).* Ligand **1b** (130 mg, 0.59 mmol, 2.1 equiv) was dissolved in MeOH (~30 mL), and (NBu$_4$)[ReOCl$_4$] (165 mg, 0.28 mmol, 1.0 equiv) was added, which resulted in the immediate formation of bright green solution. The solution was stirred under reflux for 2 h. After the solution cooled to room temperature, **3b** precipitated as a green solid and was isolated by filtration. Recrystallization of the precipitate from MeOH gave **3b** as olive green crystals (106 mg, 69%). ^{1}H NMR (300 MHz, acetonitrile-d3) δ (ppm): 8.65 (d, J = 2.9 Hz, 1H, pyz), 8.47 (d, J = 2.8 Hz, 1H, Ar), 8.28 (dd, J = 9.1, 2.8 Hz, 1H, Ar), 8.03 (d, J = 2.9 Hz, 1H, pyz), 7.77 (dd, J = 9.0, 2.8 Hz, 1H, Ar), 7.54 (d, J = 2.9 Hz, 1H, pyz), 7.32 (d, J = 9.1 Hz, 1H, Ar), 7.15 (d, J = 2.8 Hz, 1H, pyz), 6.94 (d, J = 2.9 Hz, 1H, Ar), 6.15 (d, J = 9.1 Hz, 1H, Ar), 4.44 (s, 3H, Me), 3.33 (s, 3H, Me). IR (cm^{-1}): 3145.3 (w), 1605.6 (m), 1573.7 (m), 1502.7 (s), 1334.5 (s), 1316.8 (s), 1280.4 (s), 1254.7 (s), 1129.1 (s), 965.2 (s), 878.4 (m), 832.8 (m), 787.5 (m), 736.13 (vs), 688.3 (m), 671.5 (m), 652.4 (m), 423.4 (m). EI-MS (m/z): 674.1 [M^+]. Anal. calcd for $C_{20}H_{16}ClN_6O_7Re$ (674.03): C, 35.64; H, 2.39; N, 12.47. Found: C, 35.16; H, 2.44; N, 12.13.

*Synthesis of [ReOCl$_2$(PPh$_3$)(**1c**)] (**2c**).* Ligand **1c** (50 mg, 0.24 mmol, 1.2 equiv) was dissolved in acetonitrile (~30 mL), and [ReOCl$_3$(PPh$_3$)$_2$] (160 mg, 0.19 mmol, 1.0 equiv) was added. The suspension was stirred under reflux for 4 h, upon which the mixture turned green. After the mixture cooled to room temperature, the solvent was reduced to a small amount (~10 mL), upon which crude material of **2c** precipitated. Recrystallization of the crude material from acetonitrile gave **2c** (110 mg, 78%) as deep green crystals suitable for X-ray crystallography. ^{1}H NMR (300 MHz, acetonitrile-d3) δ 7.66 (d, J = 2.9 Hz, 1H, pyz), 7.48−7.26 (m, 15H, PPh$_3$), 6.67 (d, J = 2.9 Hz, 1H, pyz), 6.65 (d, J = 3.0 Hz, 1H, Ar), 6.61 (d, J = 9.0 Hz, 1H, Ar), 6.51 (dd, J = 9.0, 3.0 Hz, 1H, Ar), 4.08 (s, 3H, OMe), 3.69 (s, 3H, Me). ^{31}P NMR (acetonitrile-d3, 121 MHz) δ (ppm): −22.66. IR: 2955.2 (w), 1577.5 (m), 1521.9 (m), 1487.1 (m), 1425.6 (m), 1418.4 (m), 1213.9 (m), 1199.2 (s), 1087.6 (m), 961.3 (s), 812.7 (s), 691.9 (vs), 498.7 (vs). EI-MS (m/z): 707.3 [M^+ − OMe]. Anal. calcd for $C_{29}H_{26}Cl_2N_2O_3PRe$ (738.62): C, 47.16; H, 3.55; N, 3.79. Found: C, 47.86; H, 3.62; N, 3.73.

*Synthesis of [ReOCl(**1c**)$_2$] (**3c**).* Ligand **1c** (2.1 equiv, 142 mg, 0.70 mmol) was dissolved in MeOH (~30 mL), and (NBu$_4$)[ReOCl$_4$] (1.0 equiv, 194 mg, 0.33 mmol) was added, which resulted in the immediate formation of a greenish solid. The reaction solution was stirred under reflux for 2 h. After the solution cooled to room temperature, **3c** precipitated as a dark green solid and was isolated by filtration. Recrystallization of the precipitate from MeOH gave **3c** as dark green crystals (120 mg, 56%). ^{1}H NMR (300 MHz, acetonitrile-d3) δ (ppm): 7.92 (d, J = 2.8 Hz, 1H, pyz), 7.43 (d, J = 2.9 Hz, 1H, pyz), 7.21 (d, J = 3.1 Hz, 1H, Ar), 7.10 (d, J = 8.9 Hz, 1H, Ar), 7.06 (d, J = 3.1 Hz, 1H, Ar), 6.99 (dd, J = 8.9, 3.1 Hz, 1H, Ar), 6.95 (d, J = 2.8 Hz, 1H, pyz), 6.75 (d, J = 2.8 Hz, 1H, pyz), 6.55 (dd, J = 8.9, 3.1 Hz, 1H, Ar), 5.95 (d, J = 8.9 Hz, 1H, Ar), 4.46 (s, 3H, OMe), 3.85 (s, 3H, OMe), 3.70 (s, 3H, Me), 3.31 (s, 3H, Me). IR (cm^{-1}): 2929.0 (w), 1612.4 (w), 1518.8 (m), 1486.5 (m), 1460.5 (m), 1421.5 (m), 1280.7

(m), 1202.6 (s), 1040.1 (m), 942.6 (vs), 877.6 (m), 813.8 (vs), 797.4 (s), 761.2 (s), 664.8 (w), 636.0 (w), 492.8 (w), 472.5 (w), 411.8 (w). EI-MS (m/z): 644.1 [M^+]. Anal. calcd for $C_{22}H_{22}ClN_4O_4Re$ (644.09): C, 41.02; H, 3.44; N, 8.70. Found: C, 40.78; H, 3.53; N, 8.43.

Epoxidation of Cyclooctene. In a typical experiment, 2−3 mg of catalyst (1 mol %) was dissolved in 0.5 mL of the respective solvent and mixed with cyclooctene (1 equiv) and 50 μL of mesitylene (internal standard), and the mixtures were heated to the respective reaction temperatures. Then, the oxidant (3 equiv) was added. Aliquots for GC−MS (20 μL) were withdrawn with a calibrated Socorex Acura 825 10−100 μL variable volume pipet at given time intervals, quenched with MnO_2, and diluted with HPLC-grade ethyl acetate. The reaction products were analyzed by GC−MS (Agilent Technologies 7890 GC System), and the epoxide produced from each reaction mixture was quantified versus mesitylene as the internal standard.

■ ASSOCIATED CONTENT

Supporting Information

Full details on crystallographic full cyclic voltammograms for complexes **3a−c** and details on the electrochemical experimental setup; details on single crystal diffraction experiments of **2b−c** and **3b−c**. This material is available free of charge via the Internet at http://pubs.acs.org. Crystallographic data (excluding structure factors) for **2b**, **2c**, **3b** and **3c** were deposited with the Cambridge Crystallographic Data Center as supplementary publication nos. 935370 (**2c**), 935371 (**2b**), 935372 (**3c**), and 935373 (**3b**). Copies of the data can be obtained free of charge on application to The Director, CCDC, 12 Union Road, Cambridge CB2 1EZ, U.K. Fax: (internat.) +44−1223/336−033. E−mail: deposit@ccdc.cam.ac.uk.

■ AUTHOR INFORMATION

Corresponding Author

*E-mail: nadia.moesch@uni-graz.at.

Notes

The authors declare no competing financial interest.

■ ACKNOWLEDGMENTS

The authors gratefully acknowledge support from NAWI Graz.

■ REFERENCES

(1) Alajlouni, A. M.; Espenson, J. H. *J. Am. Chem. Soc.* **1995**, *117*, 9243−9250.

(2) (a) Adam, W.; Mitchell, C. M. *Angew. Chem., Int. Ed.* **1996**, *35*, 533−535. (b) Hwang, T.; Goldsmith, B. R.; Peters, B.; Scott, S. L. *Inorg. Chem.* **2013**, *52*, 13904−13917. (c) Li, S.; Zhang, B.; Kühn, F. E. *J. Organomet. Chem.* **2013**, *730*, 132−136. (d) Zhang, B.; Li, S.; Herdtweck, E.; Kühn, F. E. *J. Organomet. Chem.* **2013**, *739*, 63−68.

(3) Romão, C. C.; Kühn, F. E.; Herrmann, W. A. *Chem. Rev.* **1997**, *97*, 3197−3246.

(4) Herrmann, W. A.; Kühn, F. E. *Acc. Chem. Res.* **1997**, *30*, 169−180.

(5) Rudolph, J.; Reddy, K. L.; Chiang, J. P.; Sharpless, K. B. *J. Am. Chem. Soc.* **1997**, *119*, 6189−6190.

(6) Kühn, F. E.; Scherbaum, A.; Herrmann, W. A. *J. Organomet. Chem.* **2004**, *689*, 4149−4164.

(7) Kühn, F. E.; Santos, A. M.; Herrmann, W. A. *Dalton Trans.* **2005**, 2483−2491.

(8) (a) Herrmann, W. A.; Fischer, R. W.; Marz, D. W. *Angew. Chem., Int. Ed.* **1991**, *30*, 1638−1641. (b) Herrmann, W. A.; Kiprof, P.; Rypdal, K.; Tremmel, J.; Blom, R.; Alberto, R.; Behm, J.; Albach, R. W.; Bock, H. *J. Am. Chem. Soc.* **1991**, *113*, 6527−6537. (c) Espenson, J. H. *Chem. Commun.* **1999**, 479−488. (d) Owens, G. S.; Aries, J.; Abu-Omar, M. M. *Catal. Today.* **2000**, *55*, 317−363. (e) Oyama, S. T. *Mechanisms in Homogeneous and Heterogeneous Epoxidation Catalysis*; Elsevier: Boston, 2008. (f) Huber, S.; Cokoja, M.; Kühn, F. E. *J. Organomet. Chem.* **2014**, *751*, 25−32.

(9) Bäckvall, J.-E. *Modern Oxidation Methods*; Wiley-VCH Verlag GmbH & Co. KGaA: Weinheim, 2004.

(10) (a) Copéret, C.; Adolfsson, H.; Sharpless, K. B. *Chem. Commun.* **1997**, 1565−1566. (b) Herrmann, W. A.; Kratzer, R. M.; Ding, H.; Thiel, W. R.; Glas, H. *J. Organomet. Chem.* **1998**, *555*, 293−295. (c) Adolfsson, H.; Converso, A.; Sharpless, K. B. *Tetrahedron Lett.* **1999**, *40*, 3991−3994. (d) Adolfsson, H.; Copéret, C.; Chiang, J. P.; Yudin, A. K. *J. Org. Chem.* **2000**, *65*, 8651−8658. (e) Nabavizadeh, S. M. *Dalton Trans.* **2005**, 1644−1648. (f) Yamazaki, S. *Org. Biomol. Chem.* **2007**, *5*, 2109−2113. (g) Yamazaki, S. *Tetrahedron.* **2008**, *64*, 9253−9257. (h) Zhou, M.-D.; Yu, Y.; Capapé, A.; Jain, K. R.; Herdtweck, E.; Li, X.-R.; Li, J.; Zang, S.-L.; Kühn, F. E. *Chem.—Asian J.* **2009**, *4*, 411−418. (i) Zhou, M.-D.; Jain, K. R.; Günyar, A.; Baxter, Paul N. W.; Herdtweck, E.; Kühn, F. E. *Eur. J. Inorg. Chem.* **2009**, *2009*, 2907−2914. (j) Kiersch, K.; Li, Y.; Junge, K.; Szesni, N.; Fischer, R.; Kühn, F. E.; Beller, M. *Eur. J. Inorg. Chem.* **2012**, *2012*, 5972−5978. (k) Zhang, Y.; Li, Z.; Cao, X.; Zhao, J. *J. Mol. Catal. A* **2013**, *366*, 149−155.

(11) Ferreira, P.; Xue, W.-M.; Bencze, É.; Herdtweck, E.; Kühn, F. E. *Inorg. Chem.* **2001**, *40*, 5834−5841.

(12) Zhou, M.-D.; Zhao, J.; Li, J.; Yue, S.; Bao, C.-N.; Mink, J.; Zang, S.-L.; Kühn, F. E. *Chem.—Eur. J.* **2007**, *13*, 158−166.

(13) (a) Rudler, H.; Ribeiro Gregorio, J.; Denise, B.; Brégeault, J.-M.; Deloffre, A. *J. Mol. Catal. A* **1998**, *133*, 255−265. (b) Kühn, F. E.; Santos, A. M.; Roesky, P. W.; Herdtweck, E.; Scherer, W.; Gisdakis, P.; Yudanov, I. V.; Di Valentin, C.; Rösch, N. *Chem.—Eur. J.* **1999**, *5*, 3603−3615.

(14) Herrmann, W. A.; Fischer, R. W.; Rauch, M. U.; Scherer, W. *J. Mol. Catal.* **1994**, *86*, 243−266.

(15) (a) Bryan, J. C.; Stenkamp, R. E.; Tulip, T. H.; Mayer, J. M. *Inorg. Chem.* **1987**, *26*, 2283−2288. (b) Conry, R. R.; Mayer, J. M. *Inorg. Chem.* **1990**, *29*, 4862−4867. (c) Brown, S. N.; Mayer, J. M. *J. Am. Chem. Soc.* **1996**, *118*, 12119−12133. (d) Arterburn, J. B.; Perry, M. C.; Nelson, S. L.; Dible, B. R.; Holguin, M. S. *J. Am. Chem. Soc.* **1997**, *119*, 9309−9310.

(16) (a) Herrmann, W. A.; Rauch, M. U.; Artus, G. R. J. *Inorg. Chem.* **1996**, *35*, 1988−1991. (b) Kühn, F. E.; Rauch, M. U.; Lobmaier, G. M.; Artus, G. R. J.; Herrmann, W. A. *Chem. Ber.* **1997**, *130*, 1427−1431. (c) Dinda, S.; Drew, M. G. B.; Bhattacharyya, R. *Catal. Commun.* **2009**, *10*, 720−724. (d) Traar, P.; Schröckeneder, A.; Judmaier, M. E.; Belaj, F.; Baumgartner, J.; Sachse, A.; Mösch-Zanetti, N. C. *Eur. J. Inorg. Chem.* **2010**, *2010*, 5718−5727. (e) Terfassa, B.; Traar, P.; Volpe, M.; Mösch-Zanetti, N. C.; Raju, V. J. T.; Megersa, N.; Retta, N. *Eur. J. Inorg. Chem.* **2011**, 4434−4440.

(17) Deloffre, A.; Halut, S.; Salles, L.; Brégeault, J.-M.; Ribeiro Gregorio, J.; Denise, B.; Rudler, H. *Dalton Trans.* **1999**, 2897−2898.

(18) Lobmaier, G. M.; Frey, G. D.; Dewhurst, R. D.; Herdtweck, E.; Herrmann, W. A. *Organometallics.* **2007**, *26*, 6290−6299.

(19) Sachse, A.; Mösch-Zanetti, N. C.; Lyashenko, G.; Wielandt, J. W.; Most, K.; Magull, J.; Dall'Antonia, F.; Pal, A.; Herbst-Irmer, R. *Inorg. Chem.* **2007**, *46*, 7129−7135.

(20) Schröckeneder, A.; Traar, P.; Raber, G.; Baumgartner, J.; Belaj, F.; Mösch-Zanetti, N. C. *Inorg. Chem.* **2009**, *48*, 11608−11614.

(21) Traar, P.; Schachner, J. A.; Steiner, L.; Sachse, A.; Volpe, M.; Mösch-Zanetti, N. C. *Inorg. Chem.* **2011**, *50*, 1983−1990.

(22) Grünwald, K. R.; Saischek, G.; Volpe, M.; Mösch-Zanetti, N. C. *Inorg. Chem.* **2011**, *50*, 7162−7171.

(23) Machura, B.; Wolff, M.; Benoist, E.; Schachner, J. A.; Mösch-Zanetti, N. C. *Dalton Trans.* **2013**, *42*, 8827.

(24) Barz, M.; Rauch, M. U.; Thiel, W. R. *J. Chem. Soc., Dalton Trans.* **1997**, 2155−2162.

(25) Nawrot Modranka, J. *Polym. J. Chem.* **1988**, *62*, 417.

(26) Catalan, J.; Fabero, F.; Claramunt, R. M.; Maria, M. D. S.; Focesfoces, M. D. C.; Cano, F. H.; Martinezripoll, M.; Elguero, J.; Sastre, R. *J. Am. Chem. Soc.* **1992**, *114*, 5039−5048.

(27) (a) Pleier, A.-K.; Glas, H.; Grosche, M.; Sirsch, P.; Thiel, W. R. *Synthesis* **2001**, *2001*, 0055−0062. (b) Seubert, C. K.; Sun, Y.; Thiel, W. R. *Dalton Trans.* **2009**, 4971.
(28) Praveen Kumar, V.; Gajendra Reddy, R.; Vo, D. D.; Chakravarty, S.; Chandrasekhar, S.; Grée, R. *Bioorg. Med. Chem. Lett.* **2012**, *22*, 1439−1444.
(29) Schönberg, A.; Sina, A. *J. Am. Chem. Soc.* **1950**, *72*, 3396−3399.
(30) Chatt, J.; Rowe, G. A. *J. Chem. Soc.* **1962**, 4019.
(31) Alberto, R.; Schibli, R.; Egli, A.; Schubiger, P. A.; Herrmann, W. A.; Artus, G. R. J.; Abram, U.; Kaden, T. A. *J. Organomet. Chem.* **1995**, *493*, 119−127.
(32) (a) Machura, B.; Kruszynski, R.; Kusz, J. *Polyhedron.* **2008**, *27*, 1679−1689. (b) Herrmann, W. A. *J. Organomet. Chem.* **1995**, *500*, 149−173. (c) Fernandes, A. G.; Maia, P. I.; de Souza, E. J.; Lemos, S. S.; Batista, A. A.; Abram, U.; Ellena, J.; Castellano, E. E.; Deflon, V. M. *Polyhedron.* **2008**, *27*, 2983−2989.
(33) Machura, B.; Kusz, J. *Polyhedron.* **2008**, *27*, 923−932.
(34) (a) Mazzi, U.; Refosco, F.; Bandoli, G.; Nicolini, M. *Transition Met. Chem.* **1985**, *10*, 121−127. (b) Banbery, H. J.; Hussain, W.; Hamor, T. A.; Jones, C. J.; McCleverty, J. A. *Dalton Trans.* **1990**, 657−661.
(35) Machura, B.; Wolff, M.; Tabak, D.; Schachner, J. A.; Mösch-Zanetti, N. C. *Eur. J. Inorg. Chem.* **2012**, 3764−3773.
(36) van Kirk, C. C.; Béreau, V. M.; Abu-Omar, M. M.; Evans, D. H. *J. Electroanal. Chem.* **2003**, *541*, 31−38.
(37) (a) Carey, F. A.; Sundberg, R. J. *Advanced Organic Chemistry: Part A: Structure and Mechanisms*; Springer Science+Business Media, LLC: Norwell, 2007. (b) Nič, M.; Jirát, J.; Košata, B.; Jenkins, A.; McNaught, A. *IUPAC Compendium of Chemical Terminology*; International Union of Pure and Applied Chemistry: Research Triangle Park, NC, 2009.
(38) Hammett, L. P. *J. Am. Chem. Soc.* **1937**, *59*, 96−103.
(39) (a) Schäffner, B.; Schäffner, F.; Verevkin, S. P.; Börner, A. *Chem. Rev.* **2010**, *110*, 4554−4581. (b) Fischmeister, C.; Doucet, H. *Green Chem.* **2011**, *13*, 741. (c) Le Ravalec, V.; Dupé, A.; Fischmeister, C.; Bruneau, C. *ChemSusChem.* **2010**, *3*, 1291−1297.
(40) Sheldrick, G. M. *Acta Crystallogr., Sect. A: Found. Crystallogr.* **2008**, *64*, 112−122.